

differences in the spacing of the ligand hyperfine lines, and these predictions can be mated with experimental observations. This approach yielded a value of  $\theta = 32\text{--}36^\circ$  for the nickel-selenium complex mentioned above.<sup>24</sup>

Since our ligand hfs was not sufficiently resolved to allow observation of small deviations from the normally equal spacing of the hyperfine components, we sought to answer only one question with this technique: was there *any* reasonable value of  $\theta$  which would allow a very small value of  $A_{xx}$  to be consistent with the observed nitrogen splitting along the  $g_{xx}$  direction? An answer of *no* would mean that the  $d_{zz}$  ground state could be eliminated from consideration. Table V gives a representative sampling of the values of  $A_{yy}$ ,  $A_{xx}$ , and  $\theta$  which reproduce the observed values of  $A_1(\text{N})$  and  $A_2(\text{N})$ . These results showed that (for calculations up to  $\theta = 40^\circ$ ) the observed  $A_2(\text{N})$  splitting of 5.8 G was the *minimum* value possible for  $A_{xx}(\text{N})$ . This fact argues against the  ${}^2B_{2g}$  ground state for  $\text{NiN}_4^-$ , and, by implication,  $\text{PtN}_4^-$ , which also has a large splitting for  $A_2(\text{N})$ .

**Registry No.**  $\text{NiN}_4$ , 34303-07-6;  $\text{PdN}_4$ , 34303-08-7;  $\text{PtN}_4$ , 34341-53-2;  $\text{NiN}_4^-$ , 67904-96-5;  $\text{PdN}_4^-$ , 67904-97-6;  $\text{PtN}_4^-$ , 67904-98-7;  $\text{PtN}_4^{2-}$ , 67904-99-8.

## References and Notes

- (1) This subject has been extensively reviewed: (a) J. A. McCleverty, *Prog. Inorg. Chem.*, **10**, 49 (1968); (b) G. N. Schrauzer, *Transition Met. Chem.*, **4**, 299 (1968); (c) G. N. Schrauzer, *Acc. Chem. Res.*, **2**, 72 (1969); (d) J. A. McCleverty in "Reactions of Molecules at Electrodes", N. S. Hush, Ed., Wiley-Interscience, New York, N.Y., 1971, p 403.
- (2) A. L. Balch, F. Rohrscheid, and R. H. Holm, *J. Am. Chem. Soc.*, **87**, 2301 (1965).
- (3) A. L. Balch and R. H. Holm, *J. Am. Chem. Soc.*, **88**, 5201 (1966).
- (4) T. R. Miller and I. G. Dance, *J. Am. Chem. Soc.*, **95**, 6970 (1973).
- (5) M. G. Miles, M. B. Hursthouse, and A. G. Robinson, *J. Inorg. Nucl. Chem.*, **33**, 2015 (1971).
- (6) F. Rohrscheid, A. L. Balch, and R. H. Holm, *Inorg. Chem.*, **5**, 1542 (1966).
- (7) A. L. Balch, *J. Am. Chem. Soc.*, **91**, 1948 (1969).
- (8) L. F. Warren, *Inorg. Chem.*, **16**, 2814 (1977).
- (9) A. M. Bond, R. L. Martin, and A. F. Masters, *Inorg. Chem.*, **14**, 1432 (1975).
- (10) J. W. Lauher and J. A. Ibers, *Inorg. Chem.*, **14**, 640 (1975).
- (11) H. B. Gray, R. Williams, I. Bernal, and E. Billig, *J. Am. Chem. Soc.*, **84**, 3596 (1962).
- (12) A. Davison, N. Edelstein, R. H. Holm, and A. H. Maki, *J. Am. Chem. Soc.*, **85**, 2029 (1963).
- (13) A. Davison and R. H. Holm, *Inorg. Synth.*, **10**, 19 (1967).
- (14) H. S. Booth and N. C. Jones, *J. Ind. Eng. Chem.*, **19**, 104 (1927).
- (15) W. E. Geiger, Jr., T. E. Mines, and F. C. Senteleber, *Inorg. Chem.*, **14**, 2141 (1975).
- (16) A. H. Maki and D. H. Geske, *J. Chem. Phys.*, **30**, 1356 (1959).
- (17) D. E. Smith, *Electroanal. Chem.*, **1**, 1 (1966).
- (18) P. J. Lingane, *Inorg. Chem.*, **9**, 1162 (1970).
- (19) A. M. Bond, R. L. Martin, and A. F. Masters, *J. Electroanal. Chem.*, **72**, 187 (1976).
- (20) (a) M. Sluyters-Rehbach and J. H. Sluyters, *J. Electroanal. Chem.*, **65**, 831 (1975); (b) M. C. Hughes and D. J. Maccero, *Inorg. Chim. Acta*, **4**, 327 (1970).
- (21) R. S. Nicholson, *Anal. Chem.*, **37**, 1351 (1965).
- (22) K. S. V. Santhanam and A. J. Bard, *Electroanal. Chem.*, **4**, 215 (1970).
- (23) A. H. Maki, N. Edelstein, A. Davison, and R. H. Holm, *J. Am. Chem. Soc.*, **86**, 4580 (1964).
- (24) R. L. Shlupp, Ph.D. Thesis, University of California at Riverside, 1973.
- (25) R. Kirmse and W. Dietzsch, *J. Inorg. Nucl. Chem.*, **38**, 255 (1976).
- (26) R. D. Schmitt and A. H. Maki, *J. Am. Chem. Soc.*, **90**, 2288 (1968).
- (27) R. Kirmse, W. Dietzsch, and B. V. Solovev, *J. Inorg. Nucl. Chem.*, **39**, 1157 (1977).
- (28) A. Abraam, J. Horowitz, and M. H. L. Pryce, *Proc. R. Soc. London, Ser. A*, **230**, 169 (1955).
- (29) B. R. McGarvey, *J. Phys. Chem.*, **71**, 51 (1967).
- (30) B. R. McGarvey, *Can. J. Chem.*, **53**, 2498 (1975).
- (31) J. R. Morton, J. R. Rowlands, and D. H. Whiffen, *Natl. Phys. Lab. Bull.*, No. BPR 13 (1962).
- (32) F. C. Senteleber and W. E. Geiger, Jr., *J. Am. Chem. Soc.*, **97**, 5018 (1975).
- (33) Reference 23 gives a complete description of the equations used in these calculations. A computer program to accomplish the calculations is available either from the present authors or in ref 34.
- (34) F. C. Senteleber, Ph.D. Thesis, Southern Illinois University, Carbondale, Illinois, 1977.

Contribution from the Christopher Ingold Laboratories,  
University College, London WC1H OAJ, England

## Electronic Spectra and Resonance Raman Spectra of Mixed-Valence Linear-Chain Complexes of Platinum with 1,2-Diaminoethane

JEREMY R. CAMPBELL, ROBIN J. H. CLARK,\* and PHILIP C. TURTLE

Received July 13, 1978

The resonance Raman spectra of the mixed-valence complexes  $[\text{Pt}(\text{en})\text{X}_2][\text{Pt}(\text{en})\text{X}_4]$  and  $[\text{Pt}(\text{en})_2][\text{Pt}(\text{en})_2\text{X}_2](\text{ClO}_4)_4$ , en = 1,2-diaminoethane and X = Cl or Br, have been recorded at room temperature and at ca. 80 K by use of an excitation line whose wavenumber falls within the contours of the intense, axially polarized, mixed-valence bands of these complexes in the visible region. The resonance Raman spectra are characterized by the appearance of an intense progression  $\nu_1\nu_1$ , where  $\nu_1$  is the symmetric X-Pt<sup>IV</sup>-X stretching mode of the platinum(IV) moiety. This progression reaches  $\nu_1 = 14, 11, 14$ , and 10 for the above four complexes, respectively. Weak subsidiary progressions  $\nu_n + \nu_1\nu_1$  also appear in the spectra, where  $\nu_n$  (the enabling mode) is another Raman-active mode. From the observed progressions, the spectroscopic constants  $\omega_1$  and  $x_{11}$  are calculated for each complex. The excitation profile of the  $\nu_1$  band of all four complexes reaches a maximum near the band maximum of the axially polarized mixed-valence band of each complex, although in the case of  $[\text{Pt}(\text{en})\text{Br}_2][\text{Pt}(\text{en})\text{Br}_4]$  another maximum in the excitation profile probably occurs near 13 000  $\text{cm}^{-1}$ . The results suggest the use of the resonance Raman technique to detect and to resolve overlapped electronic absorption bands.

### Introduction

Recent resonance Raman (RR) spectroscopic studies on mixed-valence complexes have focused on the linear-chain halogen-bridged variety, viz.,  $[\text{Pt}(\text{etn})_4][\text{Pt}(\text{etn})_4\text{X}_2]\text{X}_4 \cdot n\text{H}_2\text{O}$ , etn = ethylamine,  $n = 4$  (X = Cl or Br) and  $n = 0$  (X = Br or I),<sup>1-3</sup> and  $[\text{trans-M}(\text{NH}_3)_2\text{X}_2][\text{trans-M}'(\text{NH}_3)_2\text{X}_4]$ , where M or M' = Pt or Pd and X = Cl or Br.<sup>4,5</sup> The present paper develops this subject further with a detailed study of the mixed-valence complexes  $[\text{Pt}(\text{en})\text{X}_2][\text{Pt}(\text{en})\text{X}_4]$  and  $[\text{Pt}(\text{en})_2][\text{Pt}(\text{en})_2\text{X}_2](\text{ClO}_4)_4$ , where en = 1,2-diaminoethane and X = Cl or Br. The object of the investigation is to establish the nature of the resonance Raman spectra obtained when these complexes are excited with radiation which falls within the contour of the lowest energy mixed-valence transition in each case and, thus, to provide important spectroscopic information on the complexes. The neutral ones are known to possess the linear-chain halogen-bridged structure shown in Figure 1,<sup>6</sup> the Pt<sup>II</sup>-Pt<sup>IV</sup> distance increasing in the order chloride

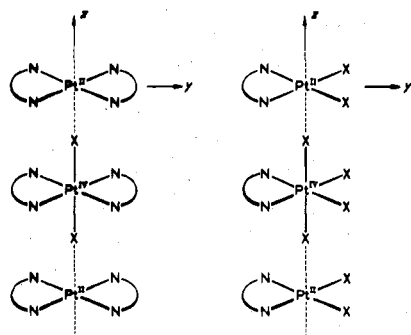


Figure 1. Structures of the complexes  $[\text{Pt}(\text{en})\text{X}_2][\text{Pt}(\text{en})\text{X}_4]$ ,  $\text{X} = \text{Cl}$  or  $\text{Br}$  (right), and those proposed for the complexes  $[\text{Pt}(\text{en})_2][\text{Pt}(\text{en})_2\text{X}_2](\text{ClO}_4)_4$ ,  $\text{X} = \text{Cl}$  or  $\text{Br}$  (left).

(5.48 Å) < bromide (5.60 Å), primarily as a consequence of an increase in the  $\text{Pt}^{\text{II}} \cdots \text{X}$  distance. These complexes possess a variety of highly anisotropic properties. In particular their electric conductance is unusual in that it suffers a continuous and reversible increase by as much as a factor of  $10^8$ – $10^9$  on application of 140-kbar pressure; the change is related to a reduction in the geometric inequivalence of the platinum(II) and platinum(IV) coordination environments brought about by compression of the chains.<sup>7,8</sup>

The structures of the cationic-chain complexes (the perchlorate salts) are deduced, from the work described herein, to have the linear-chain structures shown in Figure 1.

### Experimental Section

**Preparation of Complexes.**  $[\text{Pt}(\text{en})\text{Cl}_2][\text{Pt}(\text{en})\text{Cl}_4]$  was prepared by the method of Chugayev and Chernyaev,<sup>9</sup> using half the recommended quantity of ammonium persulfate,  $[\text{Pt}(\text{en})\text{Br}_2][\text{Pt}(\text{en})\text{Br}_4]$  by the method of Watt and McCarley,<sup>10</sup> and  $[\text{Pt}(\text{en})_2][\text{Pt}(\text{en})_2\text{Cl}_2](\text{ClO}_4)_4$  by the method of Kida.<sup>11</sup>

$[\text{Pt}(\text{en})_2][\text{Pt}(\text{en})_2\text{Br}_2](\text{ClO}_4)_4$  was prepared from the corresponding chloro complex by dissolving the latter in the minimum quantity of perchloric acid, adding concentrated HBr solution, and reducing the volume until crystals started to appear. After the solution was cooled, the resulting green-gold needles were filtered and dried in air. This procedure has also recently been adopted by Bekaroglu et al.<sup>12</sup>

**Instrumental Details.** The Raman spectra were recorded using a Spex 1401 double monochromator equipped with 1200 line  $\text{mm}^{-1}$  Bausch and Lomb gratings and a standard photon-counting detection system. Exciting radiation was provided by Coherent Radiation Models 52 and 12  $\text{Ar}^+$  ion lasers, a Model 52  $\text{Kr}^+$  ion laser, and a Model 490 tunable dye laser employing the dyes rhodamine 6G and sodium fluorescein (with cyclooctatetraene). Raman spectra at room temperature were obtained using a sample holder rotating at ca. 1600 rpm.<sup>13,14</sup> Raman spectra at ca. 80 K were obtained from alkali halide or  $\text{KClO}_4$  disks of the samples in conjunction with a glass block rotating at 1500 rpm; the rotating block refracts the laser beam rapidly across the surface of the sample in order to minimize any local heating effects.<sup>3</sup> Excitation profiles were measured with respect to the 981- $\text{cm}^{-1}$  band of  $\text{K}_2\text{SO}_4$  or the 935- $\text{cm}^{-1}$  band of  $\text{KClO}_4$ , as internal standard.

Infrared spectra were recorded on a Perkin-Elmer 225 spectrometer and on a R.I.I.C. FS 720 interferometer.

Absorption and diffuse reflectance spectra were recorded using a Cary 14 spectrometer.

### Results and Discussion

The three complexes studied are typical examples of class II mixed-valence compounds;<sup>15</sup> i.e., they are complexes in which distinct valence sites are distinguishable crystallographically but in which there is some interaction between the metal atoms at these sites. Most physical properties of such complexes are simple superpositions of the properties of the constituent complexes, with only very minor perturbations thereto. Such is the case for the infrared spectra of  $[\text{Pt}(\text{en})\text{Cl}_2][\text{Pt}(\text{en})\text{Cl}_4]$ , and  $[\text{Pt}(\text{en})\text{Br}_2][\text{Pt}(\text{en})\text{Br}_4]$  (Tables I and II) which are effectively the superpositions of those of the constituent  $\text{Pt}(\text{II})$  and  $\text{Pt}(\text{IV})$  complexes. However, for the

Table I. Wavenumbers/ $\text{cm}^{-1}$  of the Bands Observed in the IR Spectra of  $\text{Pt}(\text{en})\text{Cl}_2$ ,  $\text{Pt}(\text{en})\text{Cl}_4$ , and  $[\text{Pt}(\text{en})\text{Cl}_2][\text{Pt}(\text{en})\text{Cl}_4]$ <sup>c</sup>

$\text{Pt}(\text{en})\text{Cl}_2$ <sup>a</sup>	$[\text{Pt}(\text{en})\text{Cl}_2][\text{Pt}(\text{en})\text{Cl}_4]$	$\text{Pt}(\text{en})\text{Cl}_4$ <sup>b</sup>	assign <sup>a,b</sup>
237 sh	246 sh	248 sh	
	254 m	254 m	
282 w	277 w	298 w	Pt-Cl str
309 s	302 m		Pt-Cl str
314 s	316 s		ring skeletal
	327 m	325 m	
331 m	336 sh	335 sh	Pt-Cl str
	341 s	348 s	
464 m		468 w	Pt-N str
545 w			
	555 w	552 m	
567 s	563 w		ring skeletal
		583 w	

<sup>a</sup> R. W. Berg and K. Rasmussen, *Spectrochim. Acta, Part A*, 29a, 319 (1973). Additional bands occur at 82 (w), 91 (w), 119 (sh), 141 (m), 148 (sh), 159 (sh), and 201 (s)  $\text{cm}^{-1}$ . <sup>b</sup> This work. <sup>c</sup> w = weak, m = medium, s = strong, sh = shoulder.

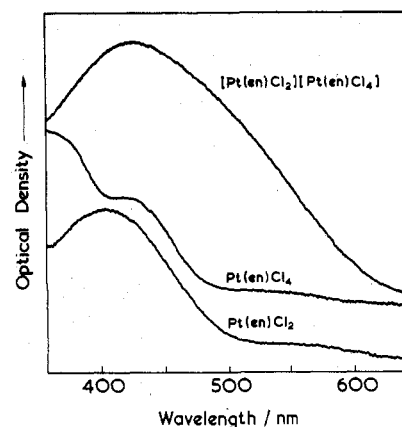


Figure 2. Diffuse reflectance spectra of the complexes  $\text{Pt}(\text{en})\text{Cl}_2$ ,  $\text{Pt}(\text{en})\text{Cl}_4$ , and  $[\text{Pt}(\text{en})\text{Cl}_2][\text{Pt}(\text{en})\text{Cl}_4]$  at 293 K.

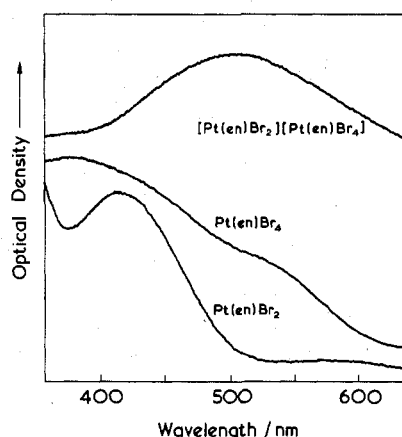


Figure 3. Diffuse reflectance spectra of the complexes  $\text{Pt}(\text{en})\text{Br}_2$ ,  $\text{Pt}(\text{en})\text{Br}_4$ , and  $[\text{Pt}(\text{en})\text{Br}_2][\text{Pt}(\text{en})\text{Br}_4]$  at 293 K.

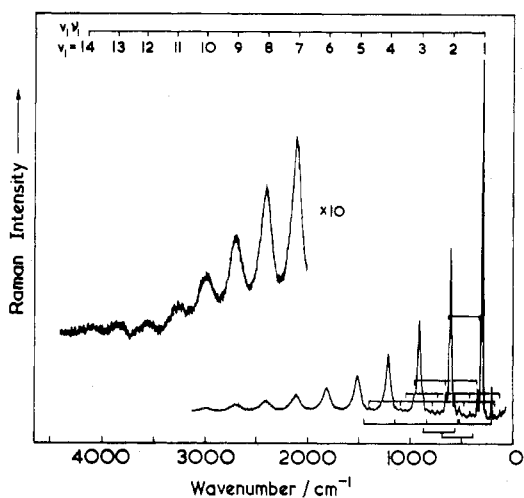
electronic and resonance Raman spectra of the mixed-valence complexes this is not the case, and accordingly these spectra are discussed in detail.

**Electronic Spectra.** The diffuse reflectance spectra of  $\text{Pt}(\text{en})\text{Cl}_2$ ,  $\text{Pt}(\text{en})\text{Cl}_4$ , and  $[\text{Pt}(\text{en})\text{Cl}_2][\text{Pt}(\text{en})\text{Cl}_4]$  are given in Figure 2, and those of  $\text{Pt}(\text{en})\text{Br}_2$ ,  $\text{Pt}(\text{en})\text{Br}_4$ , and  $[\text{Pt}(\text{en})\text{Br}_2][\text{Pt}(\text{en})\text{Br}_4]$  are given in Figure 3. In both cases, the mixed-valence complexes are deeply colored and possess a very strong asymmetric absorption band in the visible region which

**Table II.** Wavenumbers/cm<sup>-1</sup> of the Bands Observed in the IR Spectra of Pt(en)Br<sub>2</sub>, Pt(en)Br<sub>4</sub>, and [Pt(en)Br<sub>2</sub>][Pt(en)Br<sub>4</sub>]

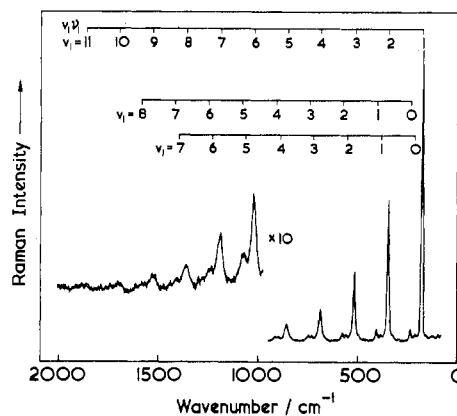
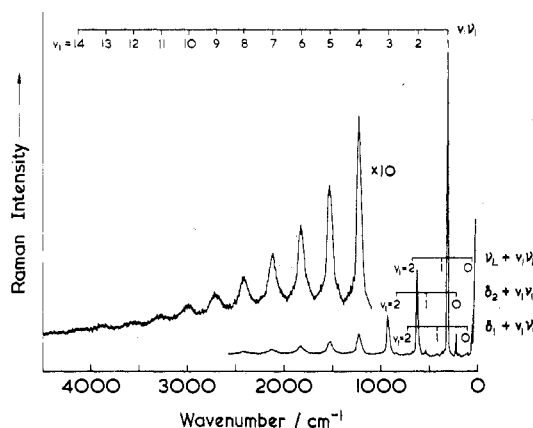
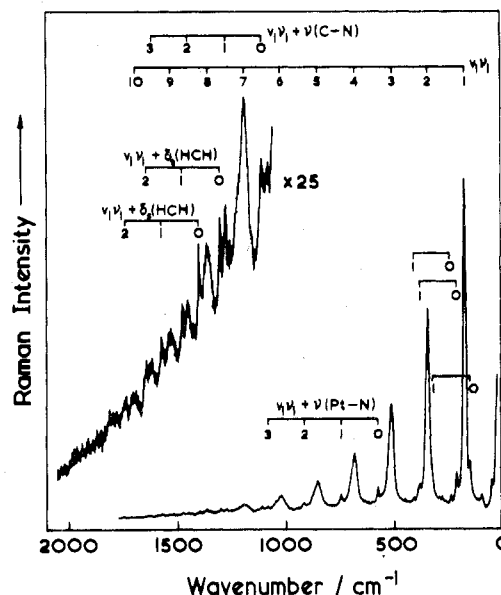
Pt(en)Br <sub>2</sub> <sup>a</sup>	[Pt(en)Br <sub>2</sub> ]- [Pt(en)Br <sub>4</sub> ]	Pt(en)Br <sub>4</sub> <sup>b</sup>	assignt
59 w	63 m	60 sh 76 m	
97 m			
119 w	102 m	106 m	
132 w	121 m		
138 w		135 w	skeletal
		147 w	
		167 w	
	179 w	179 w	
200 s		198 w	Pt-Br str
211 s	205 m		Pt-Br str
221 s	226 s	237 s	Pt-Br str
		264 w	
		288 w	
	296 sh		
317 m	312 m	316 m	ring skeletal
	334 m		
		353 w	
		376 w	
	386 m		
	396 sh	397 m	
	417 w	418 w	
	440 w		
459 m			Pt-N str

<sup>a</sup> R. W. Berg and K. Rasmussen, *Spectrochim. Acta, Part A*, 29a, 319 (1973). <sup>b</sup> This work.

**Figure 4.** Resonance Raman spectrum of the complex [Pt(en)Cl<sub>2</sub>][Pt(en)Cl<sub>4</sub>] as a KCl disk recorded with 514.5-nm excitation at ~80 K. Spectral slit width ~2 cm<sup>-1</sup>.

overlaps and completely obscures any d-d bands of either constituent ion. In the case of [Pt(en)Cl<sub>2</sub>][Pt(en)Cl<sub>4</sub>], the diffuse reflectance spectrum of the solid consists of a strong band centered at 23 500 cm<sup>-1</sup> and a shoulder at 18 900 ± 1000 cm<sup>-1</sup>. This spectrum appears to be the superposition of  $\epsilon_{\parallel}$  plus  $\epsilon_{\perp}$ , as is clear from the polarized single-crystal spectrum of the complex; this consists of<sup>16</sup> two strong bands, one polarized perpendicular to the chain axis and centered at ca. 26 500 cm<sup>-1</sup> and the other polarized parallel to the chain axis and centered at ca. 18 900 cm<sup>-1</sup>. It is this latter band which is primarily responsible for the strong, metallic reflectance of the complexes, the colors of which differ substantially from those of the corresponding powders (whose colors are more determined by diffuse than by specular reflectance). This axially polarized transition is considered<sup>2,3</sup> to be of the sort  $d_{z^2}(\text{Pt}^{\text{IV}}) \leftarrow d_{z^2}(\text{Pt}^{\text{II}})$ .

All complexes described are strongly dichroic, there being intense absorption in the visible region along the needle axis but little if any absorption perpendicular to it.

**Figure 5.** Resonance Raman spectrum of the complex [Pt(en)Br<sub>2</sub>][Pt(en)Br<sub>4</sub>] as a KBr disk recorded with 514.5-nm excitation at ~80 K. Spectral slit width ~2 cm<sup>-1</sup>.**Figure 6.** Resonance Raman spectrum of the complex [Pt(en)<sub>2</sub>][Pt(en)<sub>2</sub>Cl<sub>2</sub>](ClO<sub>4</sub>)<sub>4</sub> as a KCl disk recorded with 514.5-nm excitation at ~80 K. Spectral slit width ~2 cm<sup>-1</sup>.**Figure 7.** Resonance Raman spectrum of the complex [Pt(en)<sub>2</sub>][Pt(en)<sub>2</sub>Br<sub>2</sub>](ClO<sub>4</sub>)<sub>4</sub> as a KClO<sub>4</sub> disk recorded with 568.2-nm excitation at ~80 K. Spectral slit width ~2 cm<sup>-1</sup>.

**Resonance Raman Spectra.** The resonance Raman spectra of the complexes [Pt(en)Cl<sub>2</sub>][Pt(en)Cl<sub>4</sub>], [Pt(en)Br<sub>2</sub>][Pt(en)Br<sub>4</sub>], [Pt(en)<sub>2</sub>][Pt(en)<sub>2</sub>Cl<sub>2</sub>](ClO<sub>4</sub>)<sub>4</sub> and [Pt(en)<sub>2</sub>][Pt(en)<sub>2</sub>Br<sub>2</sub>](ClO<sub>4</sub>)<sub>4</sub> at room and liquid nitrogen temperatures are shown in Figures 4-7, respectively, and the wavenumbers

Table III. Wavenumbers/cm<sup>-1</sup> of the Raman Bands of the Complexes Pt(en)Cl<sub>2</sub>, Pt(en)Cl<sub>4</sub>, and [Pt(en)Cl<sub>2</sub>][Pt(en)Cl<sub>4</sub>]

Pt(en)-Cl <sub>2</sub> <sup>a</sup> room temp	Pt(en)-Cl <sub>4</sub> <sup>a</sup> room temp	[Pt(en)Cl <sub>2</sub> ][Pt(en)Cl <sub>4</sub> ] <sup>b</sup>		assignt
		room temp	liquid N <sub>2</sub>	
			42.0	
			49.1	
	76.7			
87.0	86.1			
94.3			95.2	
105.6				
112.0			116.2	
	129.4		123.5	
138.8	137.9			
157.9	159.0			
	170.6		169.8	
	182.0		178.3	
191.5				
	200.4			
	256.3	210.6	211.3	
		258.6	263.8	
286.3				
	298.3		295.8	
		303.5	304.9	$\nu(\text{Pt-Cl}), \nu_1$
307.8			320.0	
	335.7	337.8	341.8	$\nu(\text{Pt-Cl})$
	350.5	347.8	350.8	$\nu(\text{Pt-Cl})$
			386.4	
			421.5	$\nu_1 + 116.2$
464.0	474.0		472.8	$\nu_1 + 169.8$
			517.0	$\nu_1 + 211.3$
			528.7	
549.4	557.5			} $\nu(\text{Pt-N})$
565.7		562.8	565.8	
	574.0			
		608.8	608.7	$2\nu_1$
			624.0	$\nu_1 + 320.0$
		651.5	655.2	$\nu_1 + 350.8$
			695	$\nu_1 + 386.4$
			730	$2\nu_1 + 116.2$
			775	$2\nu_1 + 169.8$
			826	$\nu_1 + 528.7$
	868		871	$\nu_1 + \nu(\text{Pt-N})$
	912		912	$3\nu_1$
	958		960	$2\nu_1 + 350.8$
			1040	$3\nu_1 + 116.2$
			1083	$3\nu_1 + 169.8$
			1133	$2\nu_1 + 528.7$
	1214		1213	$4\nu_1$
			1389	$4\nu_1 + 169.8$
			1435	$3\nu_1 + 528.7$
		1511	1511	$5\nu_1$
		1808	1808	$6\nu_1$
		2104	2102	$7\nu_1$
		2402	2396	$8\nu_1$
		2693	2682	$9\nu_1$
			2971	$10\nu_1$
			3255	$11\nu_1$
			3541	$12\nu_1$
			3819	$13\nu_1$
			4095	$14\nu_1$

<sup>a</sup> Measured at room temperature with 647.1-nm excitation.

<sup>b</sup> Measured at room and liquid nitrogen temperatures with 514.5-nm excitation. The low-temperature spectra were obtained from a KCl disk of the complex.

and assignments of the observed bands are listed in Tables III–VI. As noted in previous studies of this sort, excitation of the complexes with radiation whose wavenumber falls within the contour of the axially polarized mixed-valence transition gives rise to RR spectra which are dominated by a progression in  $\nu_1$ , the symmetric X–Pt<sup>IV</sup>–X stretching vibration. The progression reaches, at ca. 80 K, to  $14\nu_1$ ,  $11\nu_1$ ,  $14\nu_1$ , and  $10\nu_1$  in the case of the neutral-chain chloride, the neutral-chain

Table IV. Wavenumbers/cm<sup>-1</sup> of the Raman Bands of the Complexes Pt(en)Br<sub>2</sub>, Pt(en)Br<sub>4</sub>, and [Pt(en)Br<sub>2</sub>][Pt(en)Br<sub>4</sub>]

Pt(en)-Br <sub>2</sub> <sup>a</sup> room temp	Pt(en)-Br <sub>4</sub> <sup>a</sup> room temp	[Pt(en)Br <sub>2</sub> ][Pt(en)Br <sub>4</sub> ] <sup>b</sup>		assignt
		room temp	liquid N <sub>2</sub>	
76.4				
94.6				
	99.3			
	104.8			
	115.6			
171.5				
	190.6	174.8	171.2	$\nu(\text{Pt-Br}), \nu_1$
	198.5			
	209.7	208.0	207.9	$\nu(\text{Pt-Br}), \nu_2$
217.9				
	225.1	227.0	229.7	$\nu(\text{Pt-Br}), \nu_3$
			268.4	or $\delta(\text{N-Pt-N})$
		313.0		
	319.7			
343.1				
		347.5	342.1	$2\nu_1$
		379.6	379.8	$\nu_1 + \nu_2$
	381.3			
		399.9	400.8	$\nu_1 + \nu_3$
	457.0			
		457.5		
508.8		489.4	490.0	
		521.6	512.0	$3\nu_1$
543.0	539.7			$\nu(\text{Pt-N})$
		547.2	551.5	$2\nu_1 + \nu_2$
		573.6	570.5	$2\nu_1 + \nu_3$
		619.9		
		692.2	682.0	$4\nu_1$
		723	723	$3\nu_1 + \nu_2$
		749	742	$3\nu_1 + \nu_3$
		864	851	$5\nu_1$
		896	896	$4\nu_1 + \nu_2$
			912	$4\nu_1 + \nu_3$
		1023	1021	$6\nu_1$
			1186	$7\nu_1$
			1355	$8\nu_1$
			1522	$9\nu_1$
			1691	$10\nu_1$

<sup>a</sup> Measured using 647.1-nm excitation. <sup>b</sup> Measured using 514.5-nm excitation. The low-temperature spectra were obtained from a KBr disk of the complex.

bromide, the chloride–perchlorate salt, and the bromide–perchlorate salt, respectively. The fact that the two chloride complexes have nearly identical resonance Raman spectra establishes beyond doubt that the chloride–perchlorate salt, like the neutral chloride (for which X-ray diffraction data are available),<sup>7</sup> is a chlorine-bridged chain polymer, as indicated in Figure 1. A similar situation is revealed for the two bromide complexes.

The above RR results clearly indicate that it is an axial mode and progressions based thereon which are primarily affected when the exciting radiation is brought into resonance with an axially polarized electronic band. It is this mode<sup>3</sup> which would convert the mixed-valence complex into a platinum(III)-chain transition state.

The members of the  $\nu_1\nu_1$  progression display the features typical of resonance Raman bands, viz., a continuous decrease in band intensities and a continuous increase in half-bandwidths with increase in the vibrational quantum number.<sup>13</sup> The latter effect is more dramatic at room than at liquid nitrogen temperatures (Figure 8).

The observation of a large number of overtones of a totally symmetric fundamental under resonance Raman conditions makes it possible, by standard procedures,<sup>13</sup> to determine the harmonic frequency ( $\omega_1$ ) and anharmonicity constant ( $x_{11}$ ). A plot of  $\nu(\nu_1\nu_1)/(\nu_1)$  vs.  $\nu_1$  should be a straight line of gradient

**Table V.** Wavenumbers/cm<sup>-1</sup> of the Bands Observed in the Resonance Raman Spectrum of [Pt(en)<sub>2</sub>][Pt(en)<sub>2</sub>Cl<sub>2</sub>](ClO<sub>4</sub>)<sub>4</sub> Recorded at 293 and Ca. 80 K

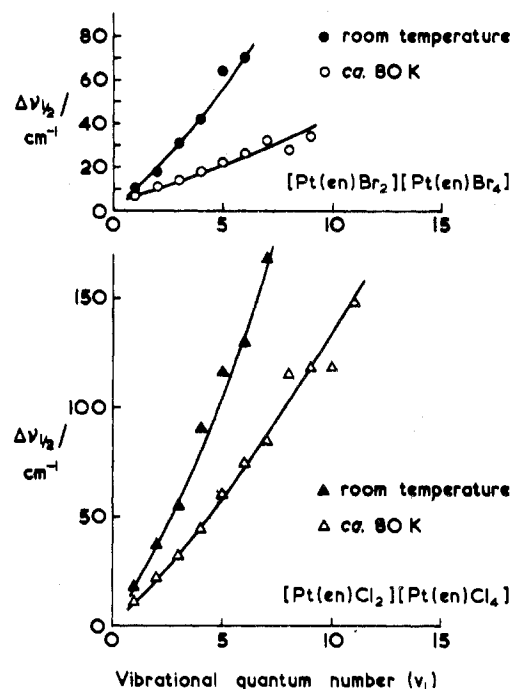
$\tilde{\nu}/\text{cm}^{-1}$		assignt
293 K <sup>a</sup>	80 K <sup>b</sup>	
	48.3	$\nu_L$
	96.6	$\delta_1$
	181.3	$\nu_2, \delta(\text{N-Pt-N})$
	215.6	$\delta_2$
312.1	308.6	$\nu(\text{Cl-Pt-Cl})_{\text{sym}}, \nu_1$
	333.4	
	356.9	$\nu_L + \nu_1$
	405.3	$\delta_1 + \nu_1$
	526.3	$\delta_2 + \nu_1$
	581.0	$\nu(\text{Pt-N})$
623.1	616.3	$2\nu_1$
	665	$\nu_L + 2\nu_1$
	715	$\delta_1 + 2\nu_1$
	833	$\delta_2 + 2\nu_1$
932.8	923	$3\nu_1$
1242	1226	$4\nu_1$
1549	1524	$5\nu_1$
1856	1822	$6\nu_1$
2160	2120	$7\nu_1$
2465	2412	$8\nu_1$
2770	2707	$9\nu_1$
	2989	$10\nu_1$
	3269	$11\nu_1$
	3553	$12\nu_1$

<sup>a</sup> M. L. Franks, Ph.D. Thesis, University of London, 1976.<sup>b</sup> KCl disk spectrum, measured with 514.5-nm excitation.**Table VI.** Wavenumbers/cm<sup>-1</sup> of the Bands Observed in the Resonance Raman Spectrum<sup>a</sup> of [Pt(en)<sub>2</sub>][Pt(en)<sub>2</sub>Br<sub>2</sub>](ClO<sub>4</sub>)<sub>4</sub> Recorded at 293 and ca. 80 K

$\tilde{\nu}/\text{cm}^{-1}$		assignt
293 K	80 K	
150.1	151.4	
173.0	173.0	$\nu_1, \nu(\text{Br-Pt-Br})_{\text{sym}}$
210	210.6	$\delta(\text{N-Pt-N})?$
	239.0	$\delta(\text{N-Pt-N})?$
324	326	$\nu_1 + 150.1/151.4$
345.8	345.7	$2\nu_1$
	388	$\nu_1 + 210/210.6$
	413	$\nu_1 + 239.0$
517	514.5	$3\nu_1$
	578.4	$\nu(\text{Pt-N})$
686.0	687.2	$4\nu_1$
	749.3	$\nu_1 + \nu(\text{Pt-N})$
846.5	856.9	$5\nu_1$
	921	$2\nu_1 + \nu(\text{Pt-N})$
1013	1023	$6\nu_1$
	1083	$3\nu_1 + \nu(\text{Pt-N})$
	1113	$\nu(\text{C-N})$
	1192	$7\nu_1$
	1280	$\nu_1 + \nu(\text{C-N})$
	1304	$\delta_t(\text{H-C-H})^b$
	1359	$8\nu_1$
	1404	$\nu_s(\text{H-C-H})^b$
	1452	$2\nu_1 + \nu(\text{C-N})$
	1476	$\nu_1 + \delta_t(\text{H-C-H})$
	1530	$9\nu_1$
	1578	$\nu_1 + \delta_s(\text{H-C-H})$
	1618	$3\nu_1 + \nu(\text{C-N})$
	1645	$2\nu_1 + \delta_t(\text{H-C-H})$
	1697	$10\nu_1$
	1748	$2\nu_1 + \delta_s(\text{H-C-H})$

<sup>a</sup> Measured with 568.2-nm excitation. The low-temperature spectrum was obtained from a KClO<sub>4</sub> disk of the complex. <sup>b</sup>  $\delta_t$  and  $\delta_s$  are the twisting and scissor or wagging modes, respectively.

$x_{11}$  and (to a first approximation) intercept  $\omega_1 + x_{11}$ . The results of such analyses on the present data are given in Table VII. In all cases, the mode which displays the RR effect is close to behaving as a simple harmonic oscillator, the average

**Figure 8.** Variation with temperature of the half-bandwidth of  $\nu_1$ -(X-Pt-X), X = Cl or Br, in [Pt(en)X<sub>2</sub>][Pt(en)X<sub>4</sub>].

value of  $x_{11}/\omega_1$  for the four complexes studied being  $-0.0026$  at 80 K.

The RR spectra of the complexes also display weak subsidiary progressions,  $\nu_n + \nu_1\nu_1$ , in which  $\nu_1$  is again the progression-forming mode and  $\nu_n$  is another Raman-active mode; viz., for [Pt(en)Cl<sub>2</sub>][Pt(en)Cl<sub>4</sub>] the progressions are based on the modes with wavenumbers of 116.2 cm<sup>-1</sup> (to  $\nu_1 = 3$ ), 169.8 cm<sup>-1</sup> (to  $\nu_1 = 4$ ), 211.3 cm<sup>-1</sup> (to  $\nu_1 = 1$ ), 320.0 cm<sup>-1</sup> (to  $\nu_1 = 1$ ), 350.8 cm<sup>-1</sup> (to  $\nu_1 = 2$ ), 386.4 cm<sup>-1</sup> (to  $\nu_1 = 1$ ), 528.7 cm<sup>-1</sup> (to  $\nu_1 = 3$ ), and 565.8 cm<sup>-1</sup> (to  $\nu_1 = 1$ ). The enabling modes (Figure 4 and Table III) for only two of the progressions have been identified: they are<sup>17</sup>  $\nu(\text{Pt-N})$  at 565.8 cm<sup>-1</sup> and  $\delta(\text{N-Pt-N})$  at 211.3 cm<sup>-1</sup>. In the case of the corresponding bromide (Figure 5 and Table IV) there are only two such subsidiary progressions:  $\nu_1\nu_1 + \nu_2$  (to  $\nu_1 = 7$ ) and  $\nu_1\nu_1 + \nu_3$  (to  $\nu_1 = 8$ ), where  $\nu_2$ , at 207.9 cm<sup>-1</sup>, and  $\nu_3$ , at 229.7 cm<sup>-1</sup>, are likely to be the nonaxial Pt-Br stretching and N-Pt-N bending modes, respectively.

For the complex [Pt(en)<sub>2</sub>][Pt(en)<sub>2</sub>Cl<sub>2</sub>](ClO<sub>4</sub>)<sub>4</sub>, additional progressions are based on  $\nu_L$ , a lattice mode at 48.3 cm<sup>-1</sup>, on  $\delta_1$ , a bending mode at 96.6 cm<sup>-1</sup>, and on  $\delta_2$ , the N-Pt-N bending mode at 215.6 cm<sup>-1</sup>; each such progression reaches to  $\nu_1 = 2$  (Figure 6 and Table V). RR progressions based on one quantum of a lattice mode have been observed previously in the case of the mixed-valence complexes of antimony.<sup>18,19</sup>

A large number of progressions are also observed for the corresponding bromide (Figure 7 and Table VI). As well as there being two progressions based on enabling modes at 210.6 and 239.0 cm<sup>-1</sup> (possibly N-Pt-N bending modes), there are further progressions based on modes at 151.4 cm<sup>-1</sup> (unassigned), 578.4 cm<sup>-1</sup> ( $\nu(\text{Pt-N})$ ), 1113 cm<sup>-1</sup> ( $\nu(\text{C-N})$ ), 1304 cm<sup>-1</sup> ( $\delta_t(\text{H-C-H})$ , twist), and 1404 cm<sup>-1</sup> ( $\delta_s(\text{H-C-H})$ , scissors or wag). The progressions based on the bands at 210.6, 239.0, and 151.4 cm<sup>-1</sup> only reached  $\nu_1 = 1$ , those based on the bands at 1304 and 1404 cm<sup>-1</sup> reached to  $\nu_1 = 2$ , and those based on the bands at 578.4 and 1113 cm<sup>-1</sup> reached to  $\nu_1 = 3$ . Progressions based on  $\nu(\text{Pt-N})$  and ligand bands in the 1000–1500-cm<sup>-1</sup> region have been observed previously in the case of other mixed-valence complexes of platinum.<sup>3</sup> Their involvement in the RR progressions can be accounted for if we assume that the lengthening of the Pt<sup>IV</sup>-X bond in the excited

Table VII. Summary of the Spectroscopic Data on the Mixed-Valence Platinum–1,2-Diaminoethane Complexes

complex	color		mixed-valence <sup>b</sup> band max/ cm <sup>-1</sup>	excitation profile max ( $\nu_1$ )/ cm <sup>-1</sup>	$\omega_1$ / cm <sup>-1</sup> (80 K)	$x_{11}$ / cm <sup>-1</sup> (80 K)	pro- gres- sion <sup>c</sup> (80 K)	$I(2\nu_1)/$ $I(\nu_1)$ max value <sup>d</sup>
	crystal <sup>a</sup>	powder						
[Pt(en)Cl <sub>2</sub> ][Pt(en) <sub>2</sub> Cl <sub>4</sub> ]	red plates	orange	23 500	18 200	307.8	-0.98	14 $\nu_1$	0.96
[Pt(en)Br <sub>2</sub> ][Pt(en) <sub>2</sub> Br <sub>4</sub> ]	green-gold plates	purple	19 000	~13 000?	171.7	-0.25	11 $\nu_1$	~0.40
[Pt(en) <sub>2</sub> ][Pt(en) <sub>2</sub> Cl <sub>2</sub> ](ClO <sub>4</sub> ) <sub>4</sub>	red needles	orange	20 000	17 000	311.3	-1.09	14 $\nu_1$	0.61
[Pt(en) <sub>2</sub> ][Pt(en) <sub>2</sub> Br <sub>2</sub> ](ClO <sub>4</sub> ) <sub>4</sub>	bronze-green needles	purple	18 400	17 700	173.2	-0.38	10 $\nu_1$	0.75

<sup>a</sup> By reflected light. <sup>b</sup> By diffuse reflectance, giving effectively the sum of  $\epsilon_{\parallel}$  plus  $\epsilon_{\perp}$ . <sup>c</sup>  $\nu_1$  is the  $\nu_{\text{sym}}(\text{X-Pt}^{\text{IV}}-\text{X})$  fundamental. <sup>d</sup> The maximum value of  $I(2\nu_1)/I(\nu_1)$  does not necessarily occur for an exciting line of wavenumber equal to that of the maximum of the  $\nu_1$  band excitation profile.

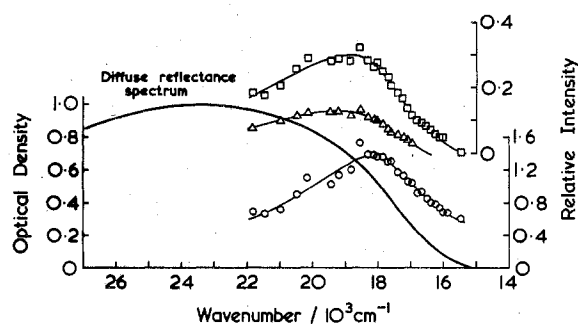


Figure 9. Excitation profiles of the  $\nu_1$  (O),  $2\nu_1$  (□), and  $3\nu_1$  (Δ) bands of the complex [Pt(en)Cl<sub>2</sub>][Pt(en)Cl<sub>4</sub>];  $\nu_1$  is the  $\nu_{\text{sym}}(\text{Cl-Pt}^{\text{IV}}-\text{Cl})$  band at 305 cm<sup>-1</sup>.

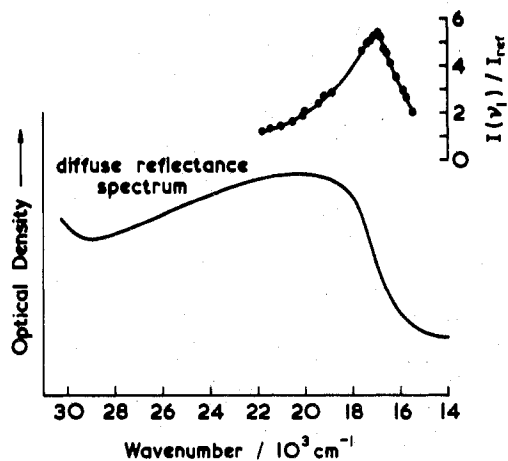


Figure 10. Diffuse reflectance spectrum of [Pt(en)<sub>2</sub>][Pt(en)<sub>2</sub>Cl<sub>2</sub>](ClO<sub>4</sub>)<sub>4</sub>, together with the excitation profiles of the  $\nu_1$ ,  $\nu_{\text{sym}}(\text{Cl-Pt}^{\text{IV}}-\text{Cl})$  band at 309 cm<sup>-1</sup>.

state causes some slight rearrangement in the positions of the ligands about the Pt atoms (possibly due to some relief of steric strain).

**Excitation Profiles.** The excitation profiles of the  $\nu_1$ ,  $2\nu_1$ , and  $3\nu_1$  bands for [Pt(en)Cl<sub>2</sub>][Pt(en)Cl<sub>4</sub>] are plotted in Figure 9; these reach maxima at  $18\,200 \pm 300$  cm<sup>-1</sup>,  $18\,700 \pm 500$  cm<sup>-1</sup>, and  $19\,200 \pm 700$  cm<sup>-1</sup>, respectively (it is not certain whether the apparently progressive shift in the maximum to higher wavenumbers with increase in  $\nu_1$  is significant). It is immediately clear that these excitation profiles maximize at the same wavenumber (within experimental error) as that of the axially polarized mixed-valence transition which is the resonant electronic transition, at  $18\,900 \pm 700$  cm<sup>-1</sup>.<sup>16</sup> The close relation between resonance Raman and electronic spectroscopy is thus made clear, as is the power of the technique of plotting excitation profiles as a means of resolving overlapped electronic absorption bands of different polarizations.

The excitation profile of the  $\nu_1$  band of [Pt(en)<sub>2</sub>][Pt(en)<sub>2</sub>Cl<sub>2</sub>](ClO<sub>4</sub>)<sub>4</sub>, Figure 10, reaches a maximum at 17 000

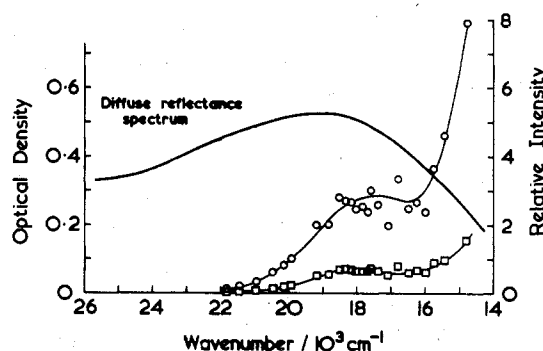


Figure 11. Excitation profiles of the  $\nu_1$  (O) and  $2\nu_1$  (□) bands of the complex [Pt(en)Br<sub>2</sub>][Pt(en)Br<sub>4</sub>];  $\nu_1$  is the  $\nu_{\text{sym}}(\text{Br-Pt}^{\text{IV}}-\text{Br})$  band at 175 cm<sup>-1</sup>.

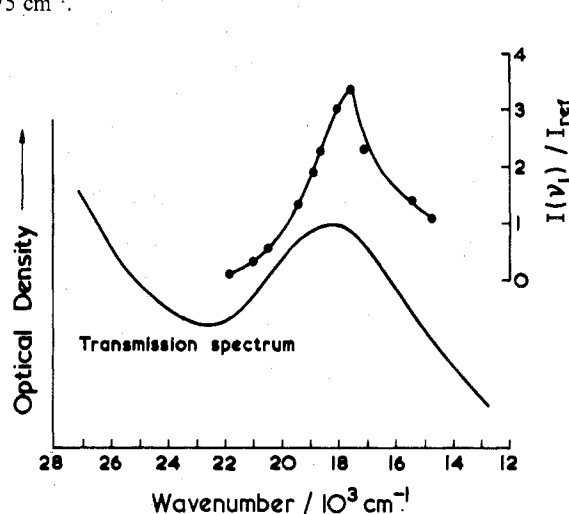


Figure 12. KClO<sub>4</sub>-disk electronic spectrum of [Pt(en)<sub>2</sub>][Pt(en)<sub>2</sub>Br<sub>2</sub>](ClO<sub>4</sub>)<sub>4</sub>, together with the excitation profile of the  $\nu_1$ ,  $\nu_{\text{sym}}(\text{Br-Pt}^{\text{IV}}-\text{Br})$ , band at 173 cm<sup>-1</sup>.

cm<sup>-1</sup>, close to that of [Pt(en)Cl<sub>2</sub>][Pt(en)Cl<sub>4</sub>]. This demonstrates the relative insensitivity of the wavenumber of the axial transition to the off-axis ligands and lends further support to the structure proposed for this complex.

The excitation profiles of the  $\nu_1$  and  $2\nu_1$  bands of [Pt(en)Br<sub>2</sub>][Pt(en)Br<sub>4</sub>] are more complicated (Figure 11). A weak maximum possibly occurs in each at ca. 17 500 cm<sup>-1</sup>, although this is not certain owing to scatter in the points. However, it seems probable (on the basis of additional studies involving 752.5- and 799.3-nm excitation) that the main maximum occurs near 13 000 cm<sup>-1</sup>. A polarized single-crystal study of this compound is clearly required.

The excitation profile of the  $\nu_1$  band of [Pt(en)<sub>2</sub>][Pt(en)<sub>2</sub>Br<sub>2</sub>](ClO<sub>4</sub>)<sub>4</sub> reaches a maximum at 17 700 cm<sup>-1</sup>, close to the electronic absorption maximum at 18 400 cm<sup>-1</sup> (Figure 12). It is this band apparently which is the resonant mixed-valence transition, for there is no lower lying shoulder as there is with the chloride complexes.

## Discussion

With this paper we have now completed RR studies on three types of mixed-valence linear-chain complexes of platinum and palladium, viz., type A,  $[\text{Pt}(\text{am})_4][\text{Pt}(\text{am})_n\text{X}_2]\text{Y}_4 \cdot n\text{H}_2\text{O}$  ( $\text{am} = \text{en}$ ,  $\text{Y} = \text{X} = \text{Cl}$  or  $\text{Br}$ ,  $n = 4$ ,  $\text{Y} = \text{X} = \text{Br}$  or  $\text{I}$ ,  $n = 0$ ;  $\text{am} = \text{en}/2$ ,  $\text{X} = \text{Cl}$  or  $\text{Br}$ ,  $n = 0$ ,  $\text{Y} = [\text{ClO}_4]^-$ ), type B,  $[\text{trans-M}(\text{NH}_3)_2\text{X}_2][\text{trans-M}'(\text{NH}_3)_2\text{X}_4]$  ( $\text{M}$  or  $\text{M}' = \text{Pd}$  or  $\text{Pt}$ ,  $\text{X} = \text{Cl}$  or  $\text{Br}$ ), and type C,  $[\text{Pt}(\text{en})\text{X}_2][\text{Pt}(\text{en})\text{X}_4]$  ( $\text{X} = \text{Cl}$  or  $\text{Br}$ ). It seems appropriate, therefore, to offer some general comments on these three types of mixed-valence complex and also to compare the RR results with those obtained previously<sup>18,19</sup> on Sb(III)/Sb(V) systems.

Perhaps the most notable difference between the antimony and platinum systems is in the relative strengths of the RR effects, viz., shorter progressions in the antimony case as well as much lower scattering cross sections. This difference probably has several causes, such as the presence of six equivalent Sb(V) atoms surrounding each Sb(III) atom whereas there are only two (approximately) equivalent Pt(IV) atoms around each Pt(II) atom; this would lead to smaller excited-state metal-halogen bond length changes in the antimony case. Moreover, there is no direct halogen bridging between the Sb(III) and Sb(V) atoms so that the phonon-assisted electron transfer affects a greater number of metal-halogen bond lengths than does the electron transfer in the platinum case. We might classify the antimony complexes as outer-sphere and the platinum ones as inner-sphere mixed-valence complexes.

On comparing the properties of the three types of platinum mixed-valence complexes it becomes obvious that types A and C are similar, with respect both to their electronic absorption and to their RR spectroscopy. Most of the chloro complexes exist as red-brown needles (giving orange-red powders) and the bromo complexes exist as green-gold needles (giving purple powders). Both chloro and bromo complexes give relatively simple RR spectra which are dominated by progressions in the axial  $\text{X-M}^{\text{IV}}\text{-X}$  stretching mode. In contrast, the complexes belonging to type B exhibit more complex RR behavior because of the major involvement in the electronic transition of the off-axis metal-ligand stretching modes. The reason for this difference has been given at some length previously<sup>3</sup> and it suffices to say that it arises from a different ordering in this case of the orbitals which are principally metal d in character.

With two exceptions, none of the types A, B, or C complexes so far investigated shows any kind of structure in the bands arising from the axial breathing mode. Since this mode does not seem to be coupled strongly with other modes of the Pt(IV) moiety, structure arising from the distribution of the halogen isotopes should be discernible. However, only for the complexes  $[\text{Pt}(\text{en})_2][\text{Pt}(\text{en})_2\text{X}_2](\text{ClO}_4)_4$ ,  $\text{X} = \text{Cl}$  or  $\text{Br}$ , is there any

indication of such structure, with the bands being skewed to higher Raman shifts. The lack of isotopic structure to the  $\nu_1$  band in the other cases is a matter of speculation, but we believe it may be connected with delocalization of the exciton created by the mixed-valence transition. It has been shown that the results of photoconductance experiments can best be explained if the exciton migrates along the chain.<sup>20</sup> Such migration might have an effect on the RR scattering but theoretical work on these interesting systems is obviously necessary before definite conclusions can be drawn.

The results presented in this paper have demonstrated that the characteristic form of the RR spectra can be used as a criterion for the existence of the platinum-halogen chain structure and that the plotting of RR excitation profiles can resolve overlapping absorption bands. More importantly, because of the breadth of mixed-valence absorption bands (even at temperatures as low as 4 K), RR spectroscopy remains the only technique at present for determining which of the vibrations of the complexes are involved in the electron transfer.

**Acknowledgment.** We are indebted to the Science Research Council and the University of London Intercollegiate Research Service for financial support.

**Registry No.**  $[\text{Pt}(\text{en})\text{Cl}_2][\text{Pt}(\text{en})\text{Cl}_4]$ , 50600-56-1;  $[\text{Pt}(\text{en})\text{Br}_2][\text{Pt}(\text{en})\text{Br}_4]$ , 33907-32-3;  $[\text{Pt}(\text{en})_2][\text{Pt}(\text{en})_2\text{Cl}_2](\text{ClO}_4)_4$ , 62535-06-2;  $[\text{Pt}(\text{en})_2][\text{Pt}(\text{en})_2\text{Br}_2](\text{ClO}_4)_4$ , 62535-08-4;  $\text{Pt}(\text{en})\text{Cl}_2$ , 14096-51-6;  $\text{Pt}(\text{en})\text{Cl}_4$ , 21500-56-1;  $\text{Pt}(\text{en})\text{Br}_2$ , 23858-09-5;  $\text{Pt}(\text{en})\text{Br}_4$ , 41618-54-6.

## References and Notes

- (1) R. J. H. Clark, M. L. Franks, and W. R. Trumble, *Chem. Phys. Lett.*, **41**, 287 (1976).
- (2) R. J. H. Clark and M. L. Franks, *J. Chem. Soc., Dalton Trans.*, 198 (1977).
- (3) R. J. H. Clark and P. C. Turtle, *Inorg. Chem.*, **17**, 2526 (1978).
- (4) R. J. H. Clark and W. R. Trumble, *Inorg. Chem.*, **15**, 1030 (1976).
- (5) R. J. H. Clark and P. C. Turtle, *J. Chem. Soc., Dalton Trans.*, in press.
- (6) T. D. Ryan and R. E. Rundle, *J. Am. Chem. Soc.*, **83**, 2814 (1961).
- (7) K. W. Browall, J. S. Kasper, and L. V. Interrante, *Acta Crystallogr., Sect. B*, **30**, 1649 (1974).
- (8) L. V. Interrante, K. W. Browall, and F. P. Bundy, *Inorg. Chem.*, **13**, 1158 (1974).
- (9) L. Chugayev and I. Chernyaev, *Z. Anorg. Allg. Chem.*, **182**, 159 (1929).
- (10) G. W. Watt and R. E. McCarley, *J. Am. Chem. Soc.*, **79**, 4585 (1957).
- (11) S. Kida, *Bull. Chem. Soc. Jpn.*, **38**, 1804 (1965).
- (12) O. Bekaroglu, H. Breer, H. Endres, H. J. Keller, and H. N. Gung, *Inorg. Chim. Acta*, **21**, 183 (1977).
- (13) R. J. H. Clark, *Adv. Infrared Raman Spectrosc.*, **1**, 143 (1975).
- (14) W. Kiefer, *Adv. Infrared Raman Spectrosc.*, **3**, 1 (1977).
- (15) M. B. Robin and P. Day, *Adv. Inorg. Chem. Radiochem.*, **10**, 247 (1967).
- (16) S. Yamada and R. Tsuchida, *Bull. Chem. Soc. Jpn.*, **29**, 421 (1956).
- (17) K. Nakamoto, "Infrared Spectra of Inorganic and Coordination Compounds", 2nd ed., Wiley-Interscience, New York, N.Y., 1970, p 158.
- (18) R. J. H. Clark and W. R. Trumble, *J. Chem. Soc., Chem. Commun.*, 318 (1975).
- (19) R. J. H. Clark and W. R. Trumble, *J. Chem. Soc., Dalton Trans.*, 1145 (1976).
- (20) L. V. Interrante and K. W. Browall, *Inorg. Chem.*, **13**, 1162 (1974).